PCCP

Accepted Manuscript

Physical Chemistry Chemical Physics

ARTICLE

First-principle study of orthorhombic CN as a potential superhard material

Received xxth xx 20xx,
Accepted xxthxx 20xx

DOI: 10.1039/x0xx00000x

www.rsc.org/

Xiao Tang, Jian Hao*, and Yinwei Li

Using first-principle calculations, we have investigated the structural, electronic, dynamical and mechanical properties of a recently synthesized *Pnnm*-CN. Phonon dispersion and elastic constant calculations demonstrate the dynamical and mechanical stabilities of the *Pnnm* structure of CN at ambient pressure. The electronic band structure suggests that *Pnnm*-CN is an insulator with an indirect band gap of about 3.7 eV. First-principle strain-stress relations at large strains were also simulated to examine the structural and mechanical properties of *Pnnm*-CN. The established ideal tensile strength of ~ 41 GPa in the <100> direction suggests that CN is a potential superhard material. The present results provide deep insights for understanding the mechanical properties of CN and thus are helpful to explore the potential industrial applications of CN.

Introduction

Synthesizing and designing superhard materials are always of great scientific interest due to their importance in fundamental science and industrial application. It is commonly accepted that strongly covalent bonded compounds formed by light elements (B, C, N and O) have high potential to be superhard materials. β-C_3N_4, firstly proposed by Liu and Cohen[1] in 1989, was predicted to be ultra-incompressible with a bulk modulus (427 GPa) comparable to that (442 GPa[2]) of diamond. Since then, considerable efforts have been devoted to search new carbon nitrides. Theoretically, a large number of dense phases have been proposed for C_3N_4, *e.g.*, defect ZB-C_3N_4[3] (*d*-ZB-C_3N_4), α-C_3N_4,[4] pseudocubic-C_3N_4,[4] cubic-C_3N_4,[4] cubic spinel-C_3N_4,[5] *Cc*-C_3N_4,[6] *Cm*-C_3N_4,[6] *I-42m*-C_3N_4[6] and *Cmc2₁*-C_3N_4.[6] A common property shared between these C_3N_4 polymorphs is that all were predicted to be ultra-incompressible material with high bulk modulus in the range of 347-496 GPa[3-6]. Therefore, carbon nitrides are expected as competitive candidates for superhard materials. To date, numerous phases of C_3N_4 have been synthesized either as thin films (β-C_3N_4,[7] cubic-C_3N_4[8]) or as bulk forms (*d*-ZB-C_3N_4,[9] α-C_3N_4,[10] β-C_3N_4,[10] cubic-C_3N_4[11]).

In recent years, the search of superhard materials in C-N systems has been focused on stoichiometries other than C_3N_4, and various new carbon nitrides with stoichiometries CN,[6, 12-18] C_3N,[15, 19] C_3N_2,[20] CN_2[21] and $C_{11}N_4$[22] have been proposed. Among these stoichiometries CN possesses particular interest since a recent experiment has claimed the successful synthesis of CN.[23] Numerously pioneering theoretical studies[6, 12-18] on the crystal structure and mechanical property of CN have been performed before the experimental synthesis.[23] The initial predictions for CN were based on substitutional eight known *AB*-type structures, including ZB, rocksalt, rhombohedral, bct-4, H-6, GeP, β-InS and GaSe types.[12] Using the same method, more candidate structures (tetragonal rocksalt,[14] β-InS-like[15] and *cg*-CN[16]) were subsequently proposed. Among these structures, *cg*-CN was predicted to be energetically most stable at pressures up to 100 GPa.[16] Later, by using an advanced first-principle swarm structure searches, Wang[17] predicted an orthorhombic *Pnnm* structure as the energetically most stable in the pressure range of 0-100 GPa. Particularly, *Pnnm*-CN was proposed to be synthesizable at high pressure since it becomes energetically more stable with respect to the decomposition into carbon and nitrogen at pressures above 10.9 GPa.[17] The stability of the *Pnnm* structure was confirmed in the later two independent structure searches,[6, 18] in which a tetragonal *P4₂/m* structure was also predicted to be energetically more stable below ~ 22 GPa. Intriguingly, the *Pnnm* phase was subsequently synthesized in experiment at high pressure of 55 GPa and high temperature of 7000 K.[23]

The hardness of *Pnnm*-CN has been estimated from several microscopic semiempirical models (Oganov,[24, 25] Šimůnek[26] and Gao[27, 28]), and the resultant values (57-72.7 GPa[6, 17]) suggest that *Pnnm*-CN is a superhard material comparable to that of *c*-BN (47-68 GPa[29, 30]). It is noteworthy that semiempirical models are known to over-exaggerate the hardness for open framework structures,[31] which has been demonstrated in several C-N compounds. Extremely high hardness values have been estimated for *pc*-C_3N_4 (79.6 GPa[32]), β-C_3N_4 (84.5 GPa[33]), *bct*-CN_2 (77.4 GPa[21]) and *d*-BC_3 (62 GPa[34]). However, first-principle strain-stress calclations gave much lower hardness values, 45.2 GPa for *pc*-C_3N_4,[35] 60.5 GPa for β-C_3N_4,[36] 46.6 GPa for *bct*-CN_2[21] and 52.5 GPa for *d*-BC_3.[34] Here, to study the mechanical properties of *Pnnm*-CN under large structural deformations, we present a first-principle strain-stress calculation to obtain the ideal tensile and shear strengths of *Pnnm*-CN. For comparison, the synthesized *d*-ZB-C_3N_4[9] was also considered in this study. The current results show that the hardness of *Pnnm*-CN extracted from the strain-stress relation is only 41 GPa, much lower than that (62.5 GPa) estimated from semiempirical model. *Pnnm*-CN is still a superhard material and a good competitor for industrial applications.

School of Physics and Electronic Engineering, Jiangsu Normal University, Xuzhou 221116, China.
*Address correspondence to jian_hao@jsnu.edu.cn

Electronic Supplementary Information (ESI) available: [details of any supplementary information available should be included here]. See DOI: 10.1039/x0xx00000x

Computational methods

Calculations were performed using density functional theory (DFT) within the Perdew–Burke Ernzerhof (PBE)[37] generalized gradient approximation (GGA) as implemented in the Vienna *ab initio* simulation package (VASP).[38, 39] The all-electron projector augmented wave (PAW) method[37] was adopted for C and N atoms with valence electrons of $2s^22p^2$ and $2s^22p^3$, respectively. An energy cutoff of 600 eV and a Monkhorst-Pack Brillouin zone sampling grid with a resolution of 0.2 $Å^{-1}$ were used, resulting in total energy convergence better than 1 meV/atom. The phonon dispersions were computed based on the supercell approach using the PHONOPY[40] code with 2×2×3 supercell for *Pnnm*-CN. Elastic constants were calculated by the strain-stress method, and the polycrystalline bulk modulus and shear modulus were thus derived from the Voigt–Reuss–Hill averaging scheme.[41] Vickers hardness was estimated from the semiempirical microscopic hardness model by Tian et al.[27, 28] The ideal tensile and shear strengths in the various directions were obtained by calculating strain-stress relations under large structural deformation using a method described previously.[21, 42, 43] Metadynamics simulation for Pnnm-CN was applied by using the PAW method as implemented in the VASP code.[38.39] Molecular dynamics simulation for Pnnm-CN was applied by using the PAW method as implemented in the VASP code.[38.39] The simulation cell was constructed by using 48 C and 48 N atoms and *k*-mesh of 2×2×2. The canonical *NVT* (*N*-number of particles, *V*-volume, *T*-temperature) ensemble was used for molecular dynamics runs with time step of 1.0 fs.

Results and discussion

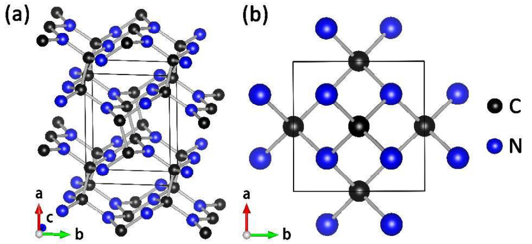

Fig. 1 (color online) Crystal structures of *Pnnm*-CN (a) and *d*-ZB-C_3N_4 (b). The black and blue spheres represent C and N atoms, respectively.

The *Pnnm* structure of CN as well as the *d*-ZB-type structure of C_3N_4 were fully geometry optimized allowing simultaneous variations of unit cell and atomic positions at selected pressures. The theoretical equilibrium properties and equation of states (EOS) were determined by fitting the total energies as functions of volume to the Murnaghan EOS.[44] The resultant equilibrium lattice parameters and atomic positions together with previous experimental[9] or theoretical[3, 17] data have been listed in Table 1. A good agreement within a maximum 6% interval can be found between the current results and previous data.[3, 9, 17] As shown in Fig. 1, The *Pnnm* structure of CN has four formula units (f.u.) in a unit cell. Each C atom in the *Pnnm* structure is bonded with three N atoms and one C atom, and each N atom is coordinated with three C atoms. The presence of sp^3-hybridized C and sp^2-hybridized N in *Pnnm*-CN is similar to that in *d*-ZB-C_3N_4, where each C atom is surrounded by four N atoms while each N atom is bonded with three C atoms (Fig. 1b). At ambient pressure, the C–C bond in *Pnnm*-CN is calculated to be 1.606 Å, which is slightly longer than that (1.535 Å) in diamond. Meanwhile, we found the C–N bond lengths (1.433-1.487 Å) in *Pnnm*-CN are slightly shorter than that (1.488 Å) in *d*-ZB-C_3N_4. The electronic band structure shows that *Pnnm*-CN is an insulator with a large indirect band gap of 3.7 eV at ambient pressure (Fig. 2a). The predicted gap for *Pnnm*-CN is larger than that (2.9 eV[4]) of cubic-C_3N_4 and is comparable to that (3.85 eV[4]) of α-C_3N_4.

Table 1 The calculated equilibrium structural parameters of *Pnnm*-CN and *d*-ZB-C_3N_4 at ambient pressure.

Phase	Lattice parameters (Å)	Volume ($Å^3$/atom)	Atomic coordinates
Pnnm-CN	*a* = 5.335 *b* = 3.952 *c* = 2.374	6.257 (6.12[a])	C (4*g*) (0.354,0.548,0.5) N (4*g*) (0.798,0.768,0.5)
d-ZB-C_3N_4	*a* = 3.455 (3.52[b]) (3.43[c])	5.89 (6.23[b]) (5.76[c])	C (3*c*) (0.5,0.5,0) N (4*e*) (0.254,0.254,0.254)

[a]Reference[17] [b]Reference[9] [c]Reference[3]

The structural stability of *Pnnm*-CN at ambient pressure has been examined by calculating the phonon dispersion and elastic constants. No imaginary phonon frequencies are observed in the whole Brillouin zone (Fig. 2b) and the whole set of elastic constants satisfy the mechanical stability criteria for an orthorhombic crystal[45] (Table 2). These results indicate the dynamical and mechanical stabilities of the *Pnnm* structure at ambient pressure. To further investigate the stability of *Pnnm*-CN under ambient pressure and temperature, metadynamics simulations were performed at 1 bar and *T* = 300 K. No structural changes were observed after 2 ps indicating that *Pnnm*-CN is indeed metastable under ambient conditions. Interestingly, we found an extremely large C_{33} (1183 GPa) for *Pnnm*-CN, which is much larger than the largest component C_{11} (794 GPa) of *d*-ZB-C_3N_4 and even larger than that (C_{11} = 1050 GPa) of diamond. The large C_{33} suggests that *Pnnm*-CN is highly incompressible along the *c*-axis.

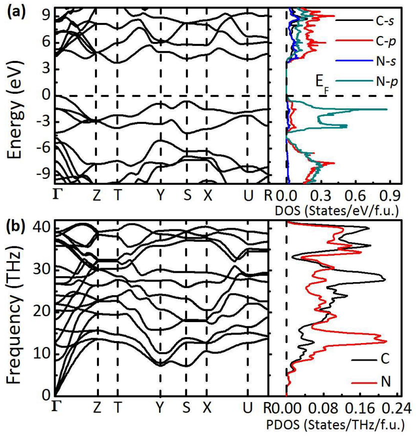

Fig. 2 (color online) The calculated electronic band structure and density of states (DOS) (a), phonon dispersion curves and phonon density of states (PDOS) (b) of *Pnnm*-CN at ambient pressure.

The bulk modulus (B_0) and shear modulus (G_0) derived from the above elastic constants are listed in Table 2. The results of *d*-ZB-C_3N_4 and diamond are also listed for comparison. The bulk modulus is calculated to be 336 GPa for *Pnnm*-CN, indicating the ultra-incompressible nature. However, the bulk modulus of *Pnnm*-CN is still lower as compared to *d*-ZB-C_3N_4 and diamond. This is understandable since *Pnnm*-CN has relatively smaller C_{11} and C_{13}. It is well-known that a superhard material should possess high bulk modulus as well as high shear modulus. Here, we also calculated the shear modulus and found that the G_0/B_0 value of *Pnnm*-CN is ~ 0.97 (Table 2). This value is identical to that calculated for *d*-ZB-C_3N_4 and lies in the range of the values (0.9-1.2) of typical covalent superhard materials, such as diamond, *c*-BN[46-48] and *c*-BC_2N.[41] Therefore, *Pnnm*-CN is expected to be a superhard material.

Table 2 The calculated elastic constants C_{ij} (GPa), bulk modulus B_0 (GPa), shear modulus G_0 (GPa), G_0/B_0 and Vickers hardness H_v of *Pnnm*-CN, *d*-ZB-C_3N_4 and diamond.

Phase	C_{11}	C_{22}	C_{33}	C_{44}	C_{55}	C_{66}	C_{12}	C_{13}	C_{23}	B_0	G_0	G_0/B_0	H_v
Pnnm-CN	506	643	1183	442	275	372	191	80	140	336	326	0.97	62.5
Pnnm-CN[a]	518	767	1227	534	277	379	203	83	201	369	351	0.95	62.3[b]
d-ZB-C_3N_4	794			431			184			387	375	0.97	63.3
c-BN[c]	820			480			190			400		0.9-1.2[d]	47-68[e]
Diamond	1050			561			124			433	519	1.20	97.8

[a]Reference[18] [b]Reference[17] [c]Reference[47] [d]Reference[46-48] [e]Reference[29, 30]

We then calculated the Vickers hardness of *Pnnm*-CN, *d*-ZB-C_3N_4 and diamond using the microscopic hardness model.[27, 28] According to this model, the hardness of a covalent crystal can be calculated from $\mathrm{H}_v^u = 740P^u(v_b^u)^{-5/3}$, where P^u and v_b^u are Mulliken overlap population and volume of u-type bond, respectively. Using this model, remarkably high hardness of 62.5 GPa was estimated for *Pnnm*-CN, in excellent agreement with a previous prediction (62.3 GPa[17]) based on the same hardness model. The hardness predicted for *Pnnm*-CN is close to that (63.3 GPa) of *d*-ZB-C_3N_4. According to this result, both *Pnnm*-CN and *d*-ZB-C_3N_4 can be classifed as superhard materials.

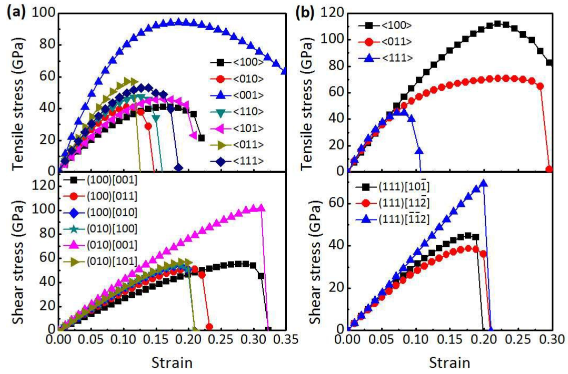

Fig. 3 **(color online)** The calculated strain-stress relation in various tensile (top panels) and shear (bottom panels) directions of *Pnnm*-CN (a) and *d*-ZB-C_3N_4 (b), respectively.

Ideal strength, the peak stress in the strain-stress curves in the weakest tensile stretch or shear slip direction, provides an assessment of the upper limit of the material strength that can be directly compared to nanoindentation measurement.[49] Therefore, strain-stress calculation is known as a method more accurate in predicting hardness of materials. Encouraged by the extremely high hardness estimated from semiempirical model, we have performed more exact first-principle strain-stress calclations on *Pnnm*-CN and *d*-ZB-C_3N_4. As shown in Fig. 3 (a), *Pnnm*-CN has high peak stresses of 41, 42, 94, 47.6, 46, 57 and 53 GPa in the <100>, <010>, <001>, <110>, <101>, <011> and <111> directions, respecitvely. The weakest peak tensile stress (*ie*. ideal tensile strength) of 41 GPa in the <100> direction for *Pnnm*-CN is comparable to the ideal tensile strength of 45 GPa estalished here for *d*-ZB-C_3N_4 (top panel of Fig. 3b), but still much smaller than that (66 GPa[50]) of *c*-BN. Meanwhile, we found the strongest peak stress of 94 GPa occurs in the <001> direction, which is larger than the ideal tensile strength (93 GPa[50]) of diamond. The presence of largest and lowest peak stresses in the <001> and <100> directions, respectively, is consistent with the large C_{33} and small C_{11} observed in the elastic constant calculations.

The weakest peak tensile stress of *Pnnm*-CN in the <100> direction suggests that the (100) planes are the easy cleavage planes. We then evaluate the shear stress response in the (100) planes by applying [001], [011] and [010] shear deformations. The lowest peak shear stress (*ie*. ideal shear strength) of 51 GPa in the (100)[011] shear direction is larger than the ideal tensile strength. We also examined the shear stress in the (010) secondly easy cleavage planes, and the resultant minimal peak shear stress is 54 GPa in the (010)[100] shear direction. The ideal tensile and shear strengths are both above the threshold (40 GPa) for a superhard material, indicating the superhard nature of *Pnnm*-CN. Interestingly, we found the ideal shear strength ((111)[11$\bar{2}$] shear direction) of *d*-ZB-C_3N_4 is only 39 GPa, excluding it as a superhard material. The Vickers hardness of 41 GPa for *Pnnm*-CN deduced from ideal tensile strength is much lower than that (62.5 GPa) estimated by semiempicial hardness model. The discrepancy is not surprising as semiempirical model is known to over-exaggerate the hardness for open framework structures.[31] Even though the hardness is lower than *c*-BN (47-68 GPa[29, 30]), *Pnnm*-CN may still be an industrially useful material.

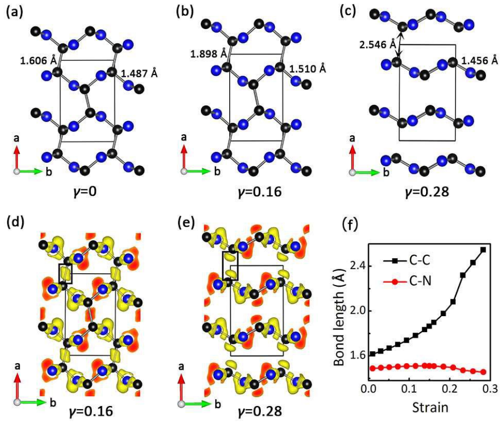

Fig. 4 **(color online)** (a-c) Structural snapshots of *Pnnm*-CN at selected stains (γ) along the <100> tensile direction. (d) and (e) are 3D electron localization function (isosurface = 0.8) of *Pnnm*-CN at strains of 0.16 and 0.28 in the <100> direction, respectively. (f) represents bond lengths under the <100> strain.

In Fig. 4, we show the structural snapshots of the *Pnnm* structure of CN at selected strains in the <100> direction to understand the local bond deformation and breaking mechanism. The *Pnnm* structure can be viewed as puckered layers of CN hexagons in the (001) planes bridged by covalent C-C bonds nearly along the <100> direction. We found that the ideal tensile strength of *Pnnm*-CN coincides with the onset of sudden increase of elongation of C-C bonds at the tensile strain of 0.17 (Fig. 4f). However, it is surprisingly to find that the <100> tensile stress decreases very gradually over a wide range of tensile strain (0.17-0.21) past the peak tensile stress, which is different from the sharply drop behaviour found in superhard *c*-BN[50] and diamond.[50] Interesingly, hardening of C-N bonds was found with the continuely weakened C-C bond as indicated by the slightly decreased C-N bond length from the strain of 0.15 (Fig. 4f). This is understandable since each C atom is surrounded by three N atoms and one C atom, formimg three C-N and one C-C bonds. C atoms will be inevitably dragged close to N atom as a result of the weakening of the C-C bonds. As shown in Fig. 4 (e), the C-C bonds have been broken at the strains after 0.21 in view of the absence of ELF between two neighboring C atoms. These results demonstrate that C-C bonds are the main load bearing component relating to the structural stability of *Pnnm*-CN.

Conclusion

In summary, we have performed systematic first-principle calculations to study the structural, electronic, dynamical and mechanical properties of *Pnnm*-CN. Results show that *Pnnm*-CN synthesized at high pressure and temperature is dynamically and mechanically stable at ambient pressure established from the phonon dispersion and elastic constants calculations. Significantly, *Pnnm*-CN possesses high ideal tensile (41 GPa) and shear (51 GPa) strengths obtained from the strain-stress relations, indicating its superhard nature. Analysis of the local bond deformation at the strains in the <100> direction demonstrates that C-C bonds are the main component relating to the structural stability of *Pnnm*-CN. We believe that the current study will advance the understanding of properties of *Pnnm*-CN and simulate its potential industrial applications.

Acknowledgements

J. H. and Y. L. acknowledge the funding supports from the National Natural Science Foundation of China under Grant Nos. 11404148 and 11204111, the Natural Science Foundation of Jiangsu province under Grant No. BK20130223, and Project Funded by the Priority Academic Program Development of Jiangsu Higher Education Institutions (PAPD).

References

1. A. Y. Liu and M. L. Cohen, *Science*, 1989, **245**, 841-842.
2. M. Grimsditch and A. Ramdas, *Phys. Rev. B*, 1975, **11**, 3139.
3. A. Y. Liu and R. M. Wentzcovitch, *Phys. Rev. B*, 1994, **50**, 10362.
4. D. M. Teter and R. J. Hemley, *Science*, 1996, **271**, 53-55.
5. S.-D. Mo, L. Ouyang, W. Ching, I. Tanaka, Y. Koyama and R. Riedel, *Phys. Rev. Lett.*, 1999, **83**, 5046.
6. H. Dong, A. R. Oganov, Q. Zhu and G.-R. Qian, *Scientific reports*, 2015, **5**, 9870.
7. C. Niu, Y. Z. Lu and C. M. Lieber, *Science*, 1993, **261**, 334-337.
8. Z. Zhang, H. Guo, G. Zhong, F. Yu, Q. Xiong and X. Fan, *Thin Solid Films*, 1999, **346**, 96-99.
9. J. Martin-Gil, F. J. Martin-Gil, M. Sarikaya, M. Qian, M. José-Yacamán and A. Rubio, *J. Appl. Phys.*, 1997, **81**, 2555-2559.
10. Q. Lv, C. Cao, C. Li, J. Zhang, H. Zhu, X. Kong and X. Duan, *J. Mater. Chem.*, 2003, **13**, 1241-1243.
11. P. Zinin, L. Ming, S. Sharma, S. Hong, Y. Xie, T. Irifune and T. Shinmei, 2008.
12. M. Côtéand and M. L. Cohen, *Phys. Rev. B*, 1997, **55**, 5684.
13. E. Kim, C. Chen, T. Köhler, M. Elstner and T. Frauenheim, *Phys. Rev. B*, 2001, **64**, 094107.
14. E. Kim, C. Chen, T. Köhler, M. Elstner and T. Frauenheim, *Phys. Rev. Lett.*, 2001, **86**, 652.
15. J. N. Hart, F. Claeyssens, N. L. Allan and P. W. May, *Phys. Rev. B*, 2009, **80**, 174111.
16. X. Wang, K. Bao, F. Tian, X. Meng, C. Chen, B. Dong, D. Li, B. Liu and T. Cui, *J. Chem. Phys.*, 2010, **133**, 044512.
17. X. Wang, *J. Chem. Phys.*, 2012, **137**, 184506.
18. M. Zhang, Q. Wei, H. Yan, Y. Zhao and H. Wang, *J. Phys. Chem. C*, 2014, **118**, 3202-3208.
19. É. Sandré, C. J. Pickard and C. Colliex, *Chem. Phys. Lett.*, 2000, **325**, 53-60.
20. F. Tian, J. Wang, Z. He, Y. Ma, L. Wang, T. Cui, C. Chen, B. Liu and G. Zou, *Phys. Rev. B*, 2008, **78**, 235431.
21. Q. Li, H. Liu, D. Zhou, W. Zheng, Z. Wu and Y. Ma, *PCCP*, 2012, **14**, 13081-13087.
22. Y. Ding, *Physica B*, 2012, **407**, 2282-2288.
23. E. Stavrou, S. Lobanov, H. Dong, A. R. Oganov, V. B. Prakapenka, Z. Konopkova and A. F. Goncharov, *arXiv preprint arXiv:1412.3755*, 2014.
24. A. O. Lyakhov and A. R. Oganov, *Phys. Rev. B*, 2011, **84**, 092103.
25. K. Li, X. Wang, F. Zhang and D. Xue, *Phys. Rev. Lett.*, 2008, **100**, 235504.
26. A. Šimůnek and J. Vackář, *Phys. Rev. Lett.*, 2006, **96**, 085501.
27. F. M. Gao, J. L. He, E. D. Wu, S. M. Liu, D. L. Yu, D. C. Li, S. Y. Zhang and Y. J. Tian, *Phys. Rev. Lett.*, 2003, **91**, 015502.
28. J. He, E. Wu, H. Wang, R. Liu and Y. Tian, *Phys. Rev. Lett.*, 2005, **94**, 015504.
29. Y. Zhao, D. He, L. Daemen, T. Shen, R. Schwarz, Y. Zhu, D. Bish, J. Huang, J. Zhang and G. Shen, *J. Mater. Res.*, 2002, **17**, 3139-3145.
30. R. Andrievski, *Int. J. Refract. Met. Hard Mater*, 2001, **19**, 447-452.
31. J. Tse, *J. Superhard Mater.*, 2010, **32**, 177-191.
32. J. He, L. Guo, X. Guo, R. Liu, Y. Tian, H. Wang and C. Gao, *Appl. Phys. Lett.*, 2006, **88**, 101906-101906.
33. J. Zhao and C. Fan, *Physica B*, 2008, **403**, 1956-1959.
34. M. Zhang, H. Liu, Q. Li, B. Gao, Y. Wang, H. Li, C. Chen and Y. Ma, *Phys. Rev. Lett.*, 2015, **114**, 015502.
35. Y. Zhang, H. Sun and C. Chen, *Phys. Rev. B*, 2006, **73**, 064109.
36. Y. Zhang, H. Sun and C. Chen, *Phys. Rev. B*, 2007, **76**, 144101.
37. G. Kresse and D. Joubert, *Phys. Rev. B*, 1999, **59**, 1758.
38. G. Kresse and J. Furthmüller, *Phys. Rev. B*, 1996, **54**, 11169.
39. J. P. Perdew, K. Burke and M. Ernzerhof, *Phys. Rev. Lett.*, 1996, **77**, 3865.
40. A. Togo, F. Oba and I. Tanaka, *Phys. Rev. B*, 2008, **78**, 134106.
41. R. Hill, *Proc. Phys. Soc. London, Sect. A*, 1952, **65**, 349.
42. D. Roundy, C. Krenn, M. L. Cohen and J. Morris Jr, *Phys. Rev. Lett.*, 1999, **82**, 2713.

43. M. Zhang, M. Lu, Y. Du, L. Gao, C. Lu and H. Liu, *J. Chem. Phys.*, 2014, **140**, 174505.
44. F. D. Murnaghan, *PNAS*, 1944, **30**, 244-247.
45. F. Mouhat and F.-X. Coudert, *Phys. Rev. B*, 2014, **90**, 224104.
46. H. Sun, S.-H. Jhi, D. Roundy, M. L. Cohen and S. G. Louie, *Phys. Rev. B*, 2001, **64**, 094108.
47. M. Grimsditch, E. Zouboulis and A. Polian, *J. Appl. Phys.*, 1994, **76**, 832-834.
48. E. Knittle, R. Kaner, R. Jeanloz and M. Cohen, *Phys. Rev. B*, 1995, **51**, 12149.
49. C. Krenn, D. Roundy, M. L. Cohen, D. Chrzan and J. Morris Jr, *Phys. Rev. B*, 2002, **65**, 134111.
50. Y. Zhang, H. Sun and C. Chen, *Phys. Rev. B*, 2006, **73**, 144115.